Estimation of the Source-by-Source Effect of Autorepression on Genetic Noise

Hiroyuki Okano,* Tetsuya J. Kobayashi,[†‡] Hirokazu Tozaki,[§] and Hidenori Kimura*

*Bio-Mimetic Control Research Center, The Institute of Physical and Chemical Research, RIKEN, Nagoya, Japan; [†]Research Fellow of the Japan Society for the Promotion of Science, [‡]Center for Developmental Biology, The Institute of Physical and Chemical Research, RIKEN, Kobe, Japan; and [§]ERATO Aihara Complexity Modeling Project, JST, Tokyo, Japan

ABSTRACT Transcriptional autorepression has been thought to be one of the simplest control circuits to attenuate fluctuations in gene expression. Here, we explored the effect of autorepression on fluctuations from different noise sources. We theoretically represent the fluctuations in the copy number of proteins as the sum of several terms, each of which is related to a specific noise source and expressed as the product of the source-specific fluctuations under no autorepression (path gain) and the effect of autorepression on them (loop gain). Inspection of each term demonstrates the source-independent noise-attenuating effect of autorepression as well as its source-dependent efficiency. Our experiments using a synthetic autorepression module revealed that autorepression attenuates fluctuations of various noise compositions. These findings indicate that the noise-attenuating effect of autorepression is robust against variation in noise compositions. We also experimentally estimated the loop gain for mRNA noise, demonstrating that loop gains are measurable parameters. Decomposition of fluctuations followed by experimental estimation of path and loop gains would help us to understand the noise-related feature of design principles underlying loop-containing biological networks.

INTRODUCTION

Biochemical reactions are inherently stochastic. Low abundance of some key cellular components, including DNA, mRNA, and some regulatory proteins, makes such the stochastic nature of biochemical reactions prominent, leading to large concentration fluctuations of reaction products (1–7). Because cellular functions must be executed through biochemical networks whose components are potentially noisy, cells must have evolved network architectures for efficient attenuation or utilization of noise (8–10).

Progression of biochemical reactions is under elaborate control by cellular machineries that by themselves result from biochemical reactions. Production of cellular components therefore involves a number of biochemical reactions, and consequently, a number of potential noise sources. Hence, fluctuations in the copy number of cellular components would originate from various noise sources, and the composition of fluctuations would be different from one cellular component to another. A recent study showed that both global and specific noise sources contribute to total fluctuations (11). Because such difference in a noise composition should influence the efficiency of noise attenuation by a specific control architecture, noise composition is a crucial factor for the cellular design of noise-control networks.

Noise compositions have been extensively studied for open-loop gene circuits both theoretically and experimentally (2,3,12,13). Because intracellular networks contain many loop structures, it is challenging to explore contributions from individual noise sources in loop-containing networks. In this study, we focused on a transcriptional autorepression circuit as the simplest loop-containing cellular circuit.

Transcriptional autorepression accounts for ~90% of transcriptional feedback loops in *Escherichia coli* (14). Despite its simplicity, the autorepression circuit is composed of several reactions, and thus involves several potential noise sources. The effect of autorepression on total fluctuations has been extensively studied both experimentally (15,16) and theoretically (12,17,18). There have been few studies, however, on the effect of autorepression in terms of noise composition. For instance, the previous experiments measured fluctuations in gene expression on plasmids where fluctuations in plasmid copy numbers would be dominant (15,16, 19). It is therefore still uncertain whether autorepression could act in the same manner on fluctuations of a different noise composition, such as those in chromosomal gene expression. It is also of physiological interest to examine how autorepression affects fluctuations in chromosomal gene expression in the light of its frequent appearance in *E. coli*.

For theory, Simpson and his colleagues reported a formal expression in a frequency domain for the effect of autorepression on fluctuations derived from any noise source

Submitted October 30, 2007, and accepted for publication March 18, 2008.

Hiroyuki Okano and Tetsuya J. Kobayashi contributed equally to this work. Hiroyuki Okano conducted all experimental works, and Tetsuya J. Kobayashi constructed the basic theory of the source-by-source contribution and efficiency of autorepression, and that of error estimation due to model simplification. Both of them contributed to constructing the strategy to experimentally measure the mRNA loop gain and theoretically proving the order of the efficiencies of loop gains.

Address reprint requests to H. Okano, Tel.: 81-52-736-5861; E-mail: okano@bmc.riken.jp.

Editor: Arthur Sherman.

0006-3495/08/08/1063/12 $2.00

doi: 10.1529/biophysj.107.124677

(20), and they applied it to the case of autorepression theoretically and experimentally by separately considering intrinsic and extrinsic noise sources with different simplifications (21,22). However, transduction of noise and effectiveness of a loop depend on each other since intrinsic kinetics influences both effectiveness of autorepression and transduction of intrinsic and extrinsic noise. This mutual and tangled dependency has not yet been fully understood because it requires a tangible expression by kinetic parameters of the loop-effect without simplification. Furthermore, whereas frequency of noise is more informative and robust to variations in protein populations and basal expression levels, the magnitude of noise has some compensatory advantages such as robustness to fluorescence bleaching, facility of experiments, and suitability for high-throughput analysis. Thus, it is important to decompose the magnitude of noise and specifically represent the loop-effect on it for the model of a closed-loop circuit that includes both intrinsic and extrinsic noise without any simplification.

Here we analyze the source-by-source effect of autorepression on genetic noise based on a detailed kinetic model, and demonstrate that autorepression attenuates fluctuations in gene expression irrespective of their sources. We experimentally show that the noise-attenuating effect of autorepression is robust against noise compositions. We also exemplify an experimental procedure to estimate the specific effect of autorepression on fluctuations originating from mRNA synthesis and degradation. Our theory-based experimental strategy enables us to quantify the source-by-source efficiency of a feedback loop for noise attenuation, and thus opens a way to understand the design principle of loop-containing biological networks from the viewpoint of noise.

MATERIALS AND METHODS

Plasmids and strains

Strains harboring a *tetR:egfp* fusion gene placed under wild-type or mutant $P_{\mathrm{LtetO\text{-}1}}$ promoters were constructed in several steps. The kanamycin-resistant gene *kan* was amplified from *Tn5* with primers containing an *XhoI-AvrII* cloning site and 40 nucleotide sequences complementary to immediate upstream or downstream of a *kan* open reading frame. The polymerase chain reaction product was cloned as a *SacI/KpnI* fragment into pBluescript SK (Stratagene, La Jolla, CA), resulting in the *kan* integration plasmid pHO2. The mutant *tetR* gene that encodes the $\mathrm{TetR}^{\mathrm{T40A}}$ protein (23) was made by site-directed mutagenesis of wild-type *tetR* gene using the Mutan-Super Express Km kit (Takara Bio, Shiga, Japan), and swapped with *tetR* gene in pZE11-*tetRY42A:egfp* plasmid (a kind gift from A. Becskei) (15,24), resulting in the plasmid pZE11-*tetRT40A:egfp*. The fusion gene placed under wild-type or mutant $P_{\mathrm{LtetO\text{-}1}}$ promoters was digested as an *XhoI/AvrII* fragment from the pZE11-*tetRT40A:egfp* plasmid or its derivatives where a $P_{\mathrm{LtetO\text{-}1}}$ promoter and a ribosome-binding sequence were replaced with mutant $P_{\mathrm{LtetO\text{-}1}}$ promoters (described below) and altered ribosome-binding sequences (25–27), respectively (Table 1). It was then cloned into pHO2 in the opposite direction of the *kan* gene. The resulting plasmids were inserted as a *SacI/KpnI* fragment into the chromosome of parental *E. coli* strain MC4100 by homologous recombination at the *kan* locus (28). Correspondence of each strain to a promoter and a ribosome-binding sequence is listed in Table 2.

Screening of mutant $P_{\mathrm{LtetO\text{-}1}}$ promoter

$P_{\mathrm{LtetO\text{-}1}}$ promoter from pZE21-MCS-1 (a kind gift from H. Bujard) (24) was cloned as a *XhoI/EcoRI* fragment into a derivative of pKF19k-2 vector (Takara), in which an *XhoI* site was inserted in a *SmaI* site of pKF19k-2. This plasmid was used as a template for random mutagenesis of the −10 region of $P_{\mathrm{LtetO\text{-}1}}$ using the Mutan-Super Express Km kit (Takara) and a random mutagenesis primer 5′-GATAGAGANNNNGAGCACATCAGCAGGACG-3′, where N denotes any of the four nucleotides. The $P_{\mathrm{LtetO\text{-}1}}$ promoter in pZE21-*tetRY42A:egfp* (a kind gift from A. Becskei) (15) was replaced with the mutagenized $P_{\mathrm{LtetO\text{-}1}}$ promoters, and the resultant library plasmids were used to transform the *E. coli* DH5αZ1 strain. These transformed strains were screened for mutant promoters with varied strength by inducing expression of $\mathrm{Tet}^{\mathrm{RY42A}}$:GFP (green fluorescence protein) fusion protein in Luria broth (LB) (Gibco BRL Products, Grand Island, NY) supplemented with 300 ng/ml anhydrotetracycline (atc) (Acros Organics, Geel, Belgium) and measuring GFP fluorescence by flow cytometry.

Growth conditions and measurements

Cultures inoculated from single colonies were grown overnight in LB at 25°C. The cultures were diluted 1:400 into LB, and grown for 1 h at 30°C. The cultures were further diluted 1:16 into LB supplemented with or without atc to a final concentration of 100 ng/ml for strains expressing high amount of fluorescent proteins (HOE211, HOE233, HOE256, and HOE259), and 30 ng/ml for the other strains. The cultures were further grown at 30°C for 4 h, which corresponds to ~6 cell cycles. Then, they were placed on ice for 2.5–3.5 h, during which fluorescence intensity remains almost unchanged. Cells were resuspended in phosphate-buffered saline, and placed between a coverslip and a small pad of 1.5% agarose in phosphate-buffered saline; ~30 fields were acquired at 100× magnification with the Axioplan 2 fluorescence microscope (Carl Zeiss, Tokyo, Japan), the CoolSNAP charge-coupled device camera (Nihon Roper, Chiba, Japan), and Metamorph imaging software (Molecular Devices, Tokyo, Japan). For each field, fluorescence (filter set 17) and phase contrast images were acquired. Inhomogeneous fluorescence background was subtracted at image acquisition. Inhomogeneous illumination did not contribute to >3% of total variance. Individual cells were identified by a program on Metamorph imaging software. To exclude abnormally large cells and small debris, we analyzed cells within the gate of the size between 1.5 and 4.5 arbitrary units. It should be noted that narrowing the size range for gating does not significantly affect the mean and the variance of single-cell fluorescence (Supplementary Material, Fig. S1). Still, rarely misidentified images were manually excluded. At least 1,000 cells were analyzed in the cell-size gate. The background fluorescence was determined for the parental strain MC4100, and its mean and variance were subtracted from those for strains harboring the artificial gene circuit under the assumption that GFP and background fluorescence are uncorrelated.

Measure of noise

In our experiment, the effect of autorepression is estimated at the same average copy number of proteins. Hence, dispersion of a protein distribution can be equivalently measured by variance, the Fano factor, and CV^2. We have chosen CV^2 as a measure of noise based on the following two reasons. First, each term in the expression of CV^2 is expressed by kinetic parameters directly involved in its origin. Second and more importantly, the plot of CV^2 versus mean^{-1} highlights the region of the mean copy numbers under autorepression where CV^2 values are compared.

Calculation of contributions from individual noise sources under no autorepression

CV^2 is represented in the following two ways:

$$CV^2 = c_0 + c_1 k_2 \mu^{-1} + c_2 \mu^{-1} = c_0 + c_3/k_0 + c_2 \mu^{-1}, \quad (1)$$

where μ, k_0, and k_2 denote mean fluorescence intensity, a transcription rate, and a translation rate, respectively, and c_0, c_1, c_2, c_3 denote composite parameters that contain neither k_0 nor k_2. In both expressions, the first, the second, and the third terms are originated from upstream, the mRNA, and downstream noise sources, respectively (see Theory for detail). The relative contributions from the three noise sources can be estimated from noise measurements under no autorepression with transcription rates altered (transcription experiments) or translation rates altered (translation experiment). For the transcription experiment in which k_2 is constant, the slope (S_0) and the intercept (I_0) of the fitted line in the CV^2 versus μ^{-1} plot represent $c_1k_2^{\mathrm{E}}+c_2$ and c_0, respectively, where k_2^{E} denotes the translation rate from R_{atpE} (Table 1). For the translation experiment in which k_0 is constant, the slope (S_1) and the intercept (I_1) of the fitted line in the CV^2 versus μ^{-1} plot represent c_2 and $c_0+c_3/k_0^{\mathrm{wt}}$, respectively, where k_0^{wt} denotes the transcription rate from P_{Lwt} (Table 1). By using these parameters, Eq. 1 is rewritten as follows:

$$\begin{aligned} CV^2 &= I_0 + \left\{(S_0 - S_1)k_2/k_2^{\mathrm{E}} + S_1\right\}\mu^{-1} \\ &= I_0 + (I_1 - I_0)k_0^{\mathrm{wt}}/k_0 + S_1\mu^{-1}. \end{aligned} \quad (2)$$

The ratios k_2/k_2^{E} and k_0^{wt}/k_0 are calculated as the ratios of the mean intensities for the corresponding *cis* elements. Because the I_0 and I_1 values are close to each other, the contributions from individual noise sources were calculated by using the former expression.

The effect of the transfer from the *kup* locus to the *galK* locus is estimated as follows: If the transfer, which causes the decrease in mean fluorescence, has no influence on the upstream noise source, the decrease in mean fluorescence is attributed to the decrease in the transcription rate k_0, and CV^2 is calculated according to Eq. 2. If the transfer fully affects the upstream noise source, the decrease in mean fluorescence is attributed to the decrease in the mean copy number of the upstream noise source. Since the upstream noise, c_0, is inversely proportional to the mean copy number of the upstream noise source under the assumption that that sensitivity of the transcription rate to the upstream noise source is constant (see Theory for detail), CV^2 in the case of full contribution is also calculated according to Eq. 2.

Estimation of parameters for autorepression

We assume that the steady-state transcription rate under autorepression, f, as a function of the steady-state amount of mature proteins, x, is described by the following Hill function:

$$f(x) = \frac{f_0}{r+1}\left\{r + \frac{1}{1+(x/K)^{\mathrm{n}}}\right\},$$

where f_0, r, K and n denote the transcription rate under no autorepression, a parameter related to basal transcription under full repression, the dissociation constant, and the Hill coefficient, respectively. It should be noted that the basal transcription rate is represented as ($rf_0/(r+1)$) by using these parameters. Since $f(x) = \alpha x$ holds at the steady state where α denotes the composite parameter that depends on a translation rate, a maturation rate, and the decay rates of mRNA and protein molecules. Then, the steady-state amount of mature proteins under autorepression is represented as follows:

$$x = f(x)/\alpha = \frac{f_0}{\alpha(r+1)}\left\{r + \frac{1}{1+(x/K)^{\mathrm{n}}}\right\}.$$

The steady-state amount of the mature proteins under no autorepression, $x_{\max}$, is represented as follows:

$$x_{\max} = f_0/\alpha.$$

Thus, efficiency of repression, λ, is represented as follows:

$$\lambda \equiv \frac{x}{x_{\max}} = \frac{1}{r+1}\left\{r + \frac{1}{1+(x/K)^{\mathrm{n}}}\right\}.$$

TABLE 1 TATA and RBS sequences in the $P_L tetO_2$ derivatives P_{L^*} and R_* denote names of TATA and ribosome-binding sequences, respectively; first codons are underlined

Name	Sequence (from 5′ to 3′)
P_{Lwt}	AGAGATAC
P_{L10}	AAGATAG
P_{L51}	AGAGACAC
P_{L92}	AGAGACAG
P_{L95}	AGAGAGGA
R_{wt}	ATTAAAGAGGAGAAAGGTACCATG
R_{epsilon}	ATTAACTTTATTAAAGAGGAGAAAGGTACCATG
R_{atpE}	TAATTTACCAACACTACTACGTTTTAACTGAAA-CAAACTGGAGACTGTCATG
R_{h1}	ATTAAAGAGGAGAAAAAGCTTTTG
R_{h3}	ATTAAAGAGGCGAAAAAGCTTATG

This equation is transformed as follows:

$$\ln y \equiv \ln\frac{(r+1)(1-\lambda)}{(r+1)\lambda - r} = n\ln x - n\ln K. \quad (3)$$

The experimental values were regressed by Eq. 3 for an appropriate value of parameter r.

THEORY

For our model shown in Fig. 1 *A*, its propensity function, $a(\mathbf{x})$, and stoichiometric coefficients, S, are described as

$$\begin{aligned} a(\mathbf{X}) &= (a_1(\mathbf{x}), a_2(\mathbf{x}), a_3(\mathbf{x}), a_4(\mathbf{x}), a_5(\mathbf{x}), a_6(\mathbf{x}), a_7(\mathbf{x}), a_8(\mathbf{x})) \\ &= (f(\mathbf{x}_4, \mathbf{x}_2 + \mathbf{x}_3), k_1\mathbf{x}_1, k_2\mathbf{x}_1, k_3\mathbf{x}_2, k_4\mathbf{x}_2, k_3\mathbf{x}_3, k_5, k_6\mathbf{x}_4) \end{aligned}$$

$$\begin{aligned} S &= (s_1, s_2, s_3, s_4, s_5, s_6) \\ &= \begin{pmatrix} 1 & -1 & 0 & 0 & 0 & 0 & 0 & 0 \\ 0 & 0 & 1 & -1 & -1 & 0 & 0 & 0 \\ 0 & 0 & 0 & 0 & 1 & -1 & 0 & 0 \\ 0 & 0 & 0 & 0 & 0 & 0 & 1 & -1 \end{pmatrix}, \end{aligned}$$

where $\mathbf{x}_1, \mathbf{x}_2, \mathbf{x}_3$ and $\mathbf{x}_4$ represent the copy numbers of mRNAs, immature proteins, mature proteins, and a variable that summarizes the influence of reactions upstream of transcription, respectively.

Their fluctuations around an equilibrium state, $\langle\mathbf{x}\rangle = (\langle\mathbf{x}_1\rangle, \langle\mathbf{x}_2\rangle, \langle\mathbf{x}_3\rangle, \langle\mathbf{x}_4\rangle)$, can be represented by the following Lyapunov equation:

$$AV + (VA)^{\mathrm{t}} + BB^{\mathrm{t}} = 0,$$

where A, B, and V denote a Jacobian matrix, a diffusion matrix, and a covariance matrix, respectively. The detailed derivation of this equation is found elsewhere (17,29,30).

By solving the Lyapunov equation, we can analytically derive fluctuations of any variable. For analytic calculation of the fluctuations, we define the following quantities:

1. Effective life time of component i: τ_{i}.

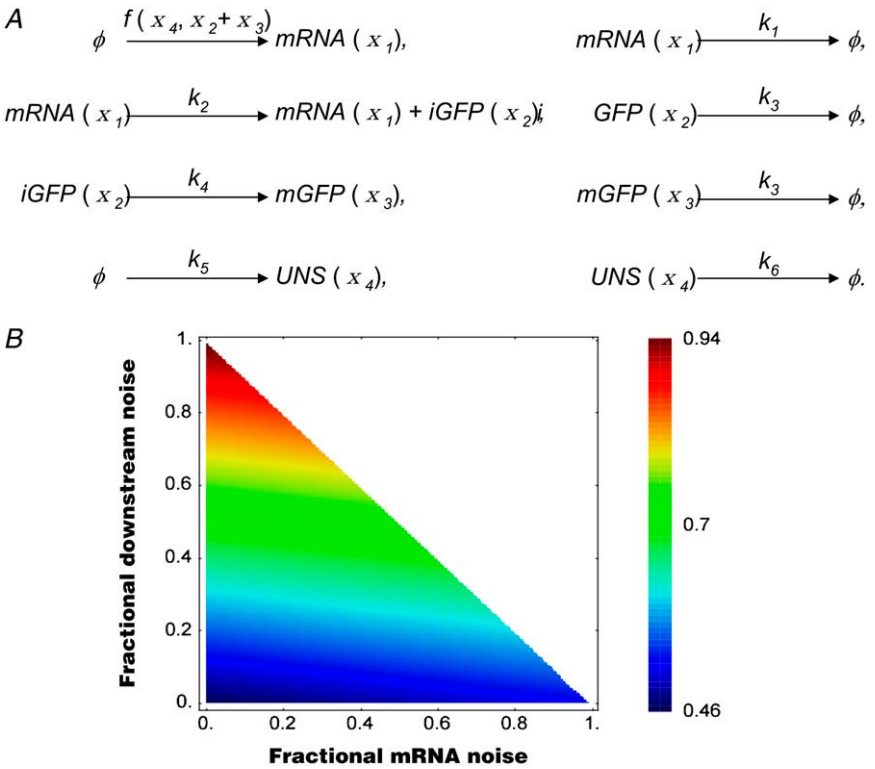

FIGURE 1 (*A*) Schematic diagram of the reaction scheme for theoretical analysis. iGFP and mGFP denote immature and mature proteins, respectively. x_1, x_2, x_3, and x_4 denote the copy number of mRNA, iGFP, mGFP, and a lumped upstream noise source, respectively. f represents the transcription rate, and k_1, k_2, k_3, k_4, k_5, and k_6 are reaction rate constants of their corresponding reactions. (*B*) Composition-dependent efficiencies of autorepression for noise attenuation. The ratio between total fluctuations under autorepression and no autorepression was numerically calculated and plotted on a noise composition plane where the x and y axes denote the fractions of fluctuations derived from mRNA and downstream noise sources, respectively. The domain that represents noise compositions is confined within a triangle defined by the x and y axes, and the dashed line. Fractional upstream noise increases in the direction from upper-right to the origin.

2. Time-averaging efficiency from component i to component j:

$$T_{\mathrm{i,j}} = \begin{cases} \dfrac{1/\tau_{\mathrm{i}}}{1/\tau_{\mathrm{i}} + 1/\tau_{\mathrm{j}}} & (i \neq j) \\ 1 & (i = j) \end{cases}.$$

3. Time-averaging efficiency between multiple components:

$$T_{\mathrm{l,k,j,i}} = T_{\mathrm{l,k}} T_{\mathrm{k,j}} T_{\mathrm{j,i}}, \quad R^{\mathrm{i}}_{\mathrm{j,k}} = \frac{1/\tau_{\mathrm{i}}}{1/\tau_{\mathrm{j}} + 1/\tau_{\mathrm{k}}}.$$

4. Time-averaging efficiency relative to component i:

$$T^{\mathrm{R}}_{\mathrm{j,k:i}} = T_{\mathrm{j,i}} T_{\mathrm{k,i}}, \quad T^{\mathrm{R}}_{\mathrm{j,k,l:i}} = T_{\mathrm{j,i}} T_{\mathrm{k,i}} T_{\mathrm{l,i}}.$$

The first two quantities were introduced previously (19), and the last two quantities are extensions of the first two ones for more than two components. In our model, $\tau_1 = 1/k_1, \tau_2 = 1/(k_3+k_4), \tau_3 = 1/k_3, \tau_4 = 1/k_6$ holds.

In addition, we define the logarithmic gains $H_{1,\mathrm{i}}$ for $i = 2, 3, 4$ as

$$H_{1,\mathrm{i}} = \left.\frac{\partial \log f(\mathbf{x}_4, \mathbf{x}_2 + \mathbf{x}_3)}{\partial \log \mathbf{x}_{\mathrm{i}}}\right|_{\mathbf{x}=\langle \mathbf{x} \rangle}.$$

It should be noted that $H_{1,2}$ and $H_{1,3}$ are negative for an autoregulatory negative feedback loop.

Furthermore, we define $\Xi_{\mathrm{all}}, \Xi_{\mathrm{iG}}, \Xi_{\mathrm{mG}}$, and Ξ_{up} as follows:

$$\Xi_{\mathrm{all}} = (1 - H_{1,2} - H_{1,3})(1 + H_{1,3}T_{1,3,2,1} - H_{1,2}T^{\mathrm{R}}_{1,2:3}),$$

$$\Xi_{\mathrm{iG}} = 1 - (H_{1,2} + H_{1,3})T^{\mathrm{R}}_{3,2:1},$$

$$\Xi_{\mathrm{mG}} = \Xi_{\mathrm{all}} + H_{1,3}(H_{1,3}T_{1,3,2,1} + (1 - H_{1,2})T^{\mathrm{R}}_{1,2:3}),$$

$$\Xi_{\mathrm{up}} = 1 - (H_{1,2}T^{\mathrm{R}}_{1,2:4} + H_{1,3}T^{\mathrm{R}}_{1,2,3:4}).$$

By using these quantities, path gains for individual noise sources are represented as follows:

$$P^{\mathrm{up}} = H^2_{1,4}(T^{\mathrm{R}}_{3,2,1:4}T^{\mathrm{R}}_{3,2,1:3}, T_{2,3,1,2}T^{\mathrm{R}}_{2,1:4}, T_{2,3}T_{3,1}T_{2,1}T_{1,4}, T^{\mathrm{R}}_{3,1:2}T^{\mathrm{R}}_{1,2:4}, T_{3,2,1,4})\langle x_4 \rangle^{-1},$$

$$P^{\mathrm{mRNA}} = (1 + R^2_{3,1})T_{3,2}T_{2,1}\langle x_1 \rangle^{-1},$$

$$P^{\mathrm{im}} = \frac{1}{2}\frac{k_4}{k_3 + k_4}\langle x_3 \rangle^{-1},$$

$$P^{\mathrm{matu}} = \frac{1}{2}\frac{k_3}{k_3 + k_4}\langle x_3 \rangle^{-1},$$

$$P^{\mathrm{dec}} = \frac{1}{2}\langle x_3 \rangle^{-1},$$

where P^{up}, P^{mRNA}, P^{im}, P^{matu}, and P^{dec} denote path gains from reactions upstream of transcription, production, and decay of the mRNA transcript, production and decay of the immature protein, maturation of the immature protein, and decay of the mature protein, respectively. A composite path gain vector for downstream noise in the main text, P^{down}, is defined as follows:

$$P^{\mathrm{down}} = (P^{\mathrm{im}}, P^{\mathrm{matu}}, P^{\mathrm{dec}}).$$

Loop gains are represented as follows:

$$G^{\mathrm{up}} = \frac{1}{\Xi_{\mathrm{all}}\Xi_{\mathrm{up}}}(1 - H_{1,2}, 1, 1, 1, 1 + H_{1,3}T^{\mathrm{R}}_{2,3;4}T_{1,3}),$$

$$G^{\mathrm{mRNA}} = \frac{1}{\Xi_{\mathrm{all}}},$$

$$G^{\mathrm{im}} = \frac{\Xi_{\mathrm{iG}}}{\Xi_{\mathrm{all}}},$$

$$G^{\mathrm{matu}} = 1,$$

$$G^{\mathrm{dec}} = \frac{\Xi_{\mathrm{mG}}}{\Xi_{\mathrm{all}}},$$

where G^{up}, G^{mRNA}, G^{im}, G^{matu}, and G^{dec} denote loop gains for reactions upstream of transcription, production and decay of the mRNA transcript, production and decay of the immature protein, maturation of the immature protein, and decay of the mature protein, respectively. A composite loop gain vector for downstream noise in the main text, G^{down}, is defined as follows:

$$G^{\mathrm{down}} = (G^{\mathrm{im}}, G^{\mathrm{matu}}, G^{\mathrm{dec}}).$$

By using these path and loop gains, CV^2. of mature GFP-fusion protein, CV^2_{mG}., is represented as

$$CV^2_{\mathrm{mG}} = \sum_{\mathrm{s}\in\{\mathrm{up,mRNA,im,matu,dec}\}} G^{\mathrm{s}} \cdot P^{\mathrm{s}},$$

where $\cdot$ represents the inner product of vectors.

Under no autorepression, elements of all loop gain vectors are shown to be one by setting $H_{1,2} = H_{1,3} = 0$. Thus, fluctuations of the mature GFP-fusion protein are represented as

$$CV^2_{\mathrm{mG}} = \sum_{\mathrm{s}\in\{\mathrm{up,mRNA,im,matu,dec}\}} 1^{\mathrm{T}} \cdot P^{\mathrm{s}},$$

where 1^{T} represents a row vector with all of its elements being one and having an appropriate dimension. For a systematic derivation of these analytical results, you will be able to consult T. J. Kobayashi, R. Tomioka, and K. Aihara (in preparation).

RESULTS AND DISCUSSION

Decomposition of noise in an autorepression-containing gene circuit

To theoretically explore the source-by-source effect of autorepression on genetic noise, we analyzed the model of bacterial gene expression (Fig. 1 *A*). In this model, we lumped possible noise sources upstream of transcription into a single one. We also included a maturation reaction for GFP protein to be fluorescent because i), most of the noise experiments used GFP or its derivatives, and ii), oxidation of the chromophore has been reported to be a slow process (31,32). We assumed that the repressor-DNA binding reaction is rapid compared to the other reactions, and that the immature protein cannot be fluorescent, but can repress its own gene expression as well as the mature protein. Under these assumptions, we analytically solved the master equation representing the reaction scheme by using the linear noise approximation method (17,29,30). The solution for total fluctuations was then decomposed into contributions from individual noise sources (T. J. Kobayashi, R. Tomioka, and K. Aihara, unpublished). In our model, fluctuations of the mature protein, denoted by a square of coefficient of variation (CV^2), are represented as the sum of the contributions from three noise sources: reactions upstream of transcription, production and decay of the mRNA transcript, and downstream reactions composed of production and decay of the immature protein, maturation of the immature protein, and decay of the mature protein. This manner of classification is based on the experimental strategy as described below. Under no autorepression, total fluctuations are represented as follows:

$$CV^2 = 1^{\mathrm{T}} \cdot P^{\mathrm{up}} + 1^{\mathrm{T}} \cdot P^{\mathrm{mRNA}} + 1^{T} \cdot P^{\mathrm{down}}, \quad (4)$$

where P^{up}, P^{mRNA}, and P^{down} represent the path gains corresponding to the upstream, the mRNA, and the downstream noise sources, respectively, 1^{T} represents a row vector with all of its elements being one and having an appropriate dimension, and $*$ represents the inner product of vectors. The elements of the three-dimensional vector P^{down} individually correspond to production and decay of the immature protein, maturation of the immature protein, and decay of the mature protein, respectively. In the presence of autorepression, total fluctuations are represented as follows:

$$CV^2 = G^{\mathrm{up}} \cdot P^{\mathrm{up}} + G^{\mathrm{mRNA}} \cdot P^{\mathrm{mRNA}} + G^{\mathrm{down}} \cdot P^{\mathrm{down}}, \quad (5)$$

where G^{up}, G^{mRNA}, and G^{down} represent the loop gains corresponding to the upstream, the mRNA, and the downstream noise sources, respectively. Loop gain thus represents the effect of autorepression on the individual noise sources. Since their values are typically different among noise sources, ''a noise composition'', which, here and hereafter, denotes a vector whose elements are relative contributions from individual noise sources under no autorepression, affects the efficiency of noise attenuation by autorepression. It can be said that autorepression attenuates fluctuations derived from noise source s if $G^{\mathrm{s}} \cdot P^{\mathrm{s}} < 1^{\mathrm{T}} \cdot P^{\mathrm{s}}$ holds where G^{s} and P^{s} represent the loop gain and the path gains corresponding to the noise source s, respectively.

It can be proved that autorepression attenuates fluctuations from any of the three noise sources (see Appendix A). Thus, even if total fluctuations under no autorepression are contributed differently from the three noise sources, they are attenuated by autorepression, provided that a decrease in a transcription rate by autorepression is compensated by raising the maximal rate of transcription (see below). It should be noted that the source-by-source noise-attenuating effect depends on how total fluctuations are classified into individual noise sources. Inspection at the level of elementary reactions revealed that autorepression has no effect on protein maturation (see Theory), suggesting that the use of a slow matu-

rating fluorescent protein such as GFP (31,32) as a reporter would underestimate the effect of autorepression on total fluctuations.

It has been reported that fluctuations of components in an open-loop circuit are decomposed in a linear fashion into elements according to their sources (13,19). Paulsson has demonstrated that noise transmission is described as the product of the magnitude of source noise, sensitivity to it, and the time-averaging effect (19). Based on this open-loop model, the source-by-source effect of autorepression has been discussed by representing the effect of an autorepression loop implicitly as the change in some key parameter. For a closed-loop circuit, it has been shown that, if a linearized model such as the Lyapunov equation or the linear Langevin equation is adopted, output noise can be formally decomposed into a linear sum of input noise multiplied by closed-loop gain for both the magnitude and the power spectrum density of output noise (17,20,22). Simpson and his colleagues used this linear relationship of the power spectrum density to experimentally evaluate the effect of autorepression on rapid intrinsic noise (21). It should be noted that the general representation of noise as a linear sum of weighted noise inputs is a consequence of linearization of noise. To reveal the ability of a given network structure to attenuate or amplify the input noise, this general representation must be interpreted in terms of the underlying kinetic parameters of the network. Our expression of output noise magnitude in Eq. 5 enables us to untangle the complicated relation between input and output noise in a closed-loop circuit by explicitly describing how the loop and path gains of both upstream and downstream noise are linked to the kinetic parameters of the circuit.

We can also demonstrate that our loop gains for intrinsic noise are reduced to those from previous studies (19,20) under additional assumptions that both maturation of proteins and decay of mRNAs are much faster than decay of proteins (see Appendix B). In Simpson's model, autorepression attenuates fluctuations from any rapid intrinsic noise sources with the same efficiencies (20,21). Thus, our analysis indicates that the difference in the lifetimes of components influence the source-by-source efficiencies of autorepression with which rapid intrinsic fluctuations are attenuated whereas the noise-attenuating effect of autorepression is robust against the lifetimes of components.

By using our analytical solution, we can further prove that the source-by-source effects of autorepression are ordered according to their efficiencies of noise attenuation (see Appendix A). Fluctuations from the upstream noise source are most efficiently attenuated; from mRNA synthesis and decay, second; and from the downstream noise source, last. Thus, noise composition affects the efficiency of noise attenuation in a manner that higher contributions from upstream noise sources enhance the attenuating effect of autorepression if the feedback gain is kept constant (Fig. 1 *B*). Since an ultrasensitive open-loop cascade inevitably accompanies large amplification of upstream fluctuations (19,33), the efficient attenuation of upstream noise by autorepression would effectively filter out fluctuations transmitted from upstream noise sources, which balances between high-sensitivity to signal and low amplification of noise. Furthermore, the effective attenuation of upstream noise explains the previous observation that autorepression drastically attenuates fluctuations of proteins expressed on plasmids (15).

Robustness of the noise-attenuating effect of autorepression against various noise compositions

We experimentally examined whether the noise-attenuating effect of autorepression is robust against variation in noise compositions as predicted theoretically. Our experimental design is based on the classification of noise sources into the following three: fluctuations upstream of transcription, fluctuations of mRNA synthesis and decay, and fluctuations downstream of mRNA synthesis and decay. Our theoretical analysis as well as previous ones predict that alteration of either transcription or translation rates gives a linear relationship between CV^2 and mean^{-1}, and contributions from the three noise sources can be estimated from the slope and the intercept of CV^2 versus mean^{-1} plot (Materials and Methods; see also Appendix C) (2,12,13).

In our theoretical analysis, the effect of autorepression is evaluated under the identical sets of kinetic parameters. This comparison is experimentally possible by assigning mean reduction due to autorepression to reduction of transcription rates. As described above, alteration of the transcription rate without autorepression should give a linear relationship between CV^2 and mean^{-1}. If CV^2 under autorepression is plotted above or below this line, it means noise amplification or attenuation by autorepression, respectively.

In our experiments, we modified a synthetic autorepression module used in the previous study (15) (Fig. 2 *A*). The previous study observed the effect of autorepression on fluctuations in gene expression on plasmids. Expression on plasmids accompanies large contributions from upstream noise sources such as plasmid copy number variation, and hence masks the noise-attenuating effect of autorepression on fluctuations from mRNA and downstream noise sources. To elevate the contributions from mRNA and downstream noise sources such as transcription and translation, we inserted the autorepression module into the *kup* locus of the *E. coli* chromosome. To increase the signal/noise ratio of the fluorescence of TetR/EGFP-repressed cells against background fluorescence, wild-type *tetR* was replaced with a mutant gene that encodes the TetR^{T40A} protein with a reduced repression activity (23).

As predicted theoretically, alteration of transcription and translation rates under no autorepression—that is, in the presence of the saturating concentration of atc—gave a linear relationship between CV^2 and mean^{-1} (Fig. 2 *B*). In the

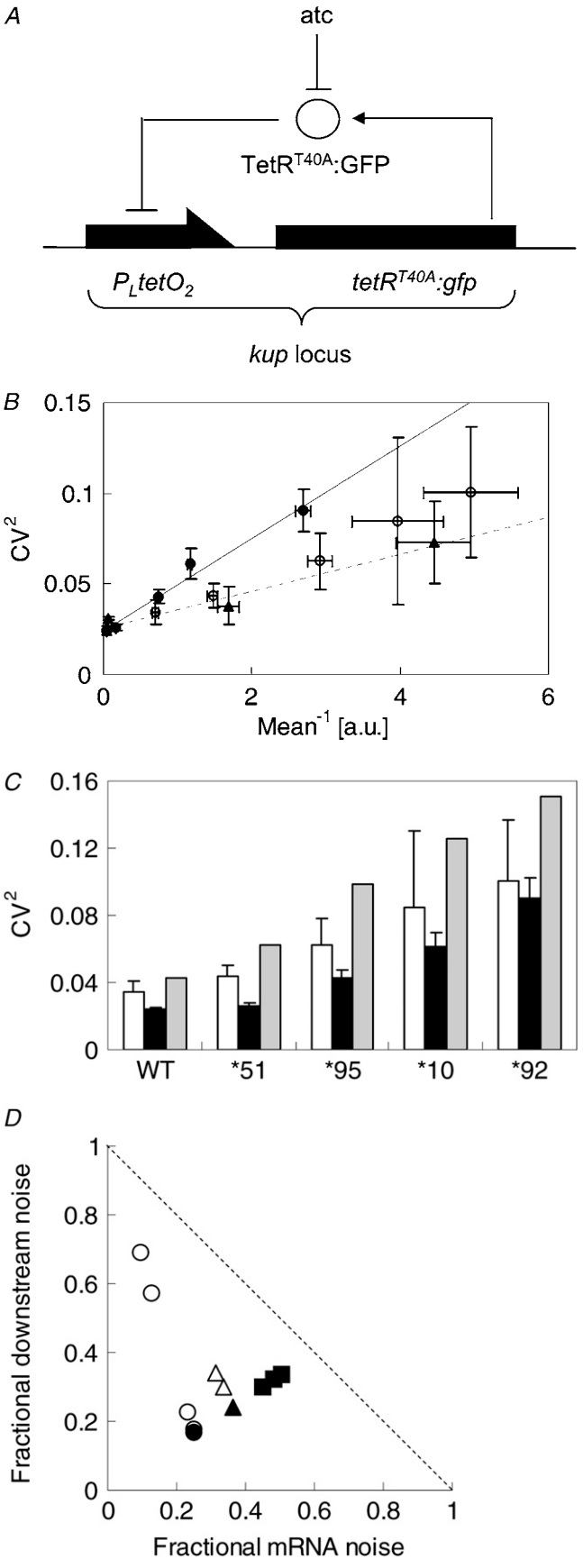

presence of autorepression—that is, in the absence of atc—CV^2 values for strains with their transcription rates altered (Fig. 2 *B*, *open circles*) were found to be below the regression line of the corresponding plot under no autorepression (Fig. 2 *B*, *solid line*), demonstrating clearly that autorepression attenuates noise in chromosomal gene expression. It should be noted that the rather subtle effect of autorepression on noise attenuation in our experimental system can only be detected by comparison under identical sets of kinetic parameters, but not by comparison in the same strain (Fig. 2 *C*). The noise-attenuating effects were also observed for all of the strains with their translation rates altered (Table 2).

We examined the relationship between noise composition and the noise-attenuating efficiency of autorepression. By using the relative kinetic parameters under autorepression, we calculated the corresponding noise composition under no autorepression (Materials and Methods; see also Appendix C). We found that the three noise sources contributed differently to the observed fluctuations depending on the transcription and translation rates (Fig. 2 *D*). Thus, the observed attenuation by autorepression of fluctuations with different noise compositions is consistent with the theoretical prediction that the noise-attenuating effect of autorepression is robust against variation in noise compositions.

Experimental estimation of the loop gain for mRNA noise

To experimentally verify the effect of autorepression further, we developed a strategy for experimental estimation of the loop gain for mRNA noise. To this purpose, we rewrite Eq. 5 as follows:

$$CV^2 = P^{\mathrm{mRNA}}\xi + \psi, \tag{6}$$

where $\xi = G^{\mathrm{mRNA}}$ and $\psi = G^{\mathrm{up}} * P^{\mathrm{up}} + G^{\mathrm{down}} * P^{\mathrm{down}}$. It should be noted that ξ and ψ are constant at the fixed average copy numbers of the mature protein molecules. Then, we can solve Eq. 6 for ξ and ψ if two sets of CV^2 and P^{mRNA} are

FIGURE 2 (*A*) Synthetic autorepression module used in this study. (*B*) The CV^2 versus mean^{-1} plot for strains with their transcription or translation rates altered. Microscopic measurements were carried out for strains with their transcription rates altered in the presence (*open circles*) or absence (*solid circle*) of autorepression, and for strains with their translation rates altered in the absence of autorepression (*solid triangles*). Curve fitting of the data under no autorepression with a function $y = ax + b$ gives $a = 0.026$ and $b = 0.025$ with a correlation coefficient $R^2 = 0.98$ for transcription series (*solid line*), and $a = 0.010$ and $b = 0.026$ with a correlation coefficient $R^2 = 0.97$ for translation series (*dashed line*). (*C*) Comparison of CV^2 values under autorepression (*open bar*) with the ones under no autorepression for the same strain (*solid bar*), or the ones under no autorepression with the same kinetic parameters (*shaded bar*), which were estimated from the fitted line in Fig. 2 *B* (*solid line*). (*D*) Noise compositions under no autorepression calculated at the parameter sets where fluctuations in the presence of autorepression were measured. The *x* and *y* axes denote the fractions of fluctuations derived from mRNA and downstream noise sources, respectively. Each point represents the noise composition for the promoter containing P_{Lwt} (*circles*), P_{L51} (*triangles*), or R_{atpE} (*closed symbols*).

TABLE 2 Effect of autorepression on noise attenuation for each strain

Strain	TATA	RBS	Locus	Mean*	Noise†
HOE259	P_{Lwt}	R_{atpE}	*kup*	0.048	0.81
HOE256	P_{Lwt}	R_{epsilon}	*kup*	0.053	0.89
HOE211	P_{Lwt}	R_{wt}	*kup*	0.062	0.88
HOE275	P_{Lwt}	R_{h3}	*kup*	0.41	0.76
HOE274	P_{Lwt}	R_{h1}	*kup*	n.d.	n.d.
HOE257	P_{L51}	R_{atpE}	*kup*	0.11	0.70
HOE253	P_{L51}	R_{epsilon}	*kup*	0.12	0.68
HOE219	P_{L51}	R_{wt}	*kup*	0.15	0.66
HOE255	P_{L95}	R_{atpE}	*kup*	0.26	0.63
HOE254	P_{L10}	R_{atpE}	*kup*	0.29	0.67
HOE258	P_{L92}	R_{atpE}	*kup*	0.54	0.66
HOE233	P_{Lwt}	R_{wt}	*galK*	0.088	0.93
HOE235	P_{L51}	R_{wt}	*galK*	n.d.	n.d.

*Ratio of the mean values in the same strain in the absence and the presence of atc.

†Ratio of variance in the absence of atc and the one under no autorepression with the same mean estimated from the fitted line (Fig. 2 *B*, *solid line*).

independently obtained under the fixed mean by altering appropriate parameters such as transcription and translation rates (see Appendix C for detail).

To alter the transcription rate without affecting efficiencies of autorepression, we transferred the autorepression module from the *kup* locus near the replication origin to the *galK* locus near the replication terminus (see Appendix D). This transfer is expected to change the transcription rate by reducing the average gene copy number in replicating the chromosome. Indeed, we observed reduction in the average amount of the mature protein by ~70%. Despite the potential influence of genomic locus on upstream noise, the effect of this transfer on upstream noise was found to be negligible in our experimental system (Fig. 3 *A*). Thus, one set of CV^2 and P^{mRNA} (denoted as CV_1^2 and P_1^{mRNA}) can be determined for the *galK* strain (HOE233), and the other set (denoted as CV_2^2 and P_2^{mRNA}) can be obtained by altering translation rates.

From noise measurements under autorepression, we obtained $CV_1^2 = 4.8\times10^{-2}$ and $CV_2^2 = 4.0\times10^{-2}$ at the mean value of the *galK* strain (HOE233), the latter of which was estimated by linear regression of a CV^2 versus mean^{-1} plot (Fig. 3 *B*). P^{mRNA} can be determined from a relative translation rate (see Eq. 2 in Materials and Methods). The relative translation rate for the translation series that gives the same mean value as the *galK* strain was estimated by fitting the autorepression curve with the Hill function (Materials and Methods) (Fig. 3 *C*). The estimated value of 2.1 for the Hill coefficient is consistent with the fact that TetR acts as a dimmer. Then, we obtained $P_1^{\mathrm{mRNA}} = 1.2\times10^{-2}$ and $P_2^{\mathrm{mRNA}} = 1.3\times10^{-3}$. Hence, the loop gain for mRNA noise was estimated as $\xi = G^{\mathrm{mRNA}} = 0.79$, demonstrating that autorepression attenuates the mRNA noise in our experimental system, as predicted by our analytical result. Our experiment not only has illustrated that the loop gains are experimentally tractable parameters, but is the first example of estimating the effect of autorepression on a specific noise

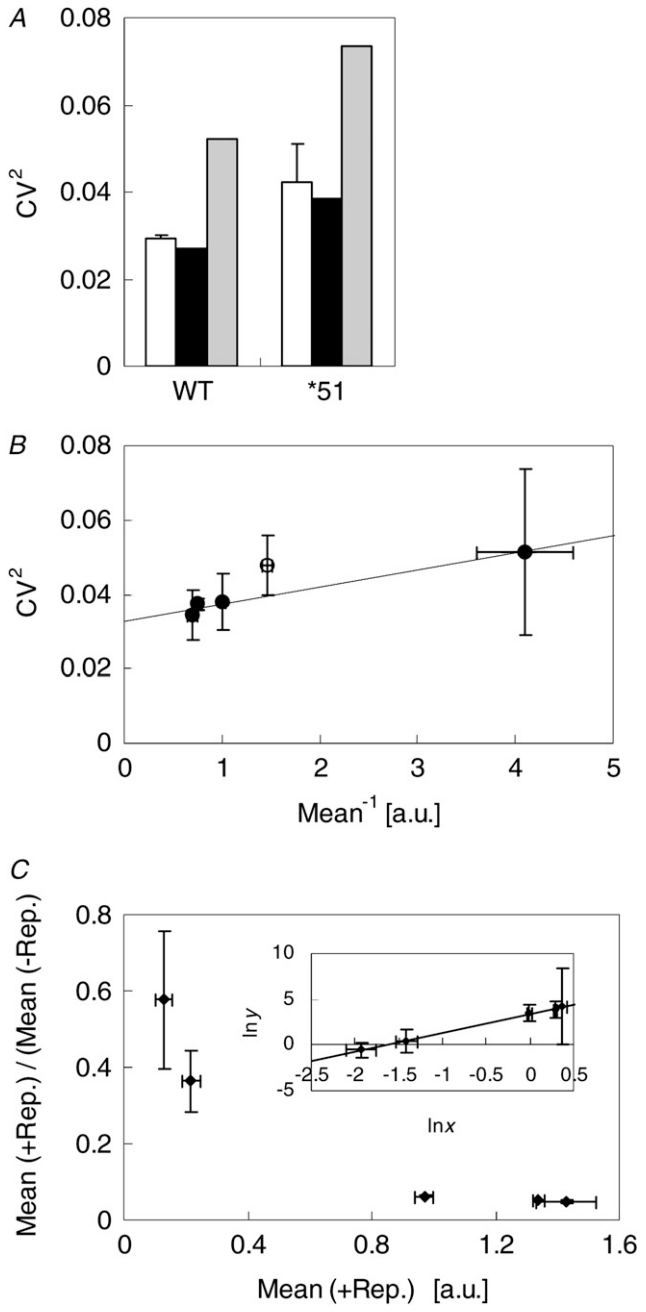

FIGURE 3 (*A*) Influence of gene loci on upstream noise. The CV^2 values under no autorepression for *galK* strains HOE233 (P_{Lwt}) and HOE235 (P_{L51}) (*open bar*) were compared with the ones calculated under assumptions that the locus-specific event responsible for reduction in the mean value does not contribute to upstream noise at all (*solid bar*), or that it contributes fully to upstream noise (*shaded bar*). (*B*) The CV^2 versus mean^{-1} plot under autorepression. Microscopic measurements were carried out in the presence of autorepression for the *galK* strain HOE233 (*open circle*), and for *kup* strains with their translation rates altered (*solid circles*). (*C*) Efficiencies of autorepression. For strains harboring the P_{Lwt} promoter and any of the RBS sequences, the mean value under autorepression divided by the one under no autorepression was plotted against the mean value under autorepression. (*Inset*) Linear regression by the Hill equation; x and y denote the steady-state fluorescence under autorepression and the parameter defined in Eq. 3, respectively (see Materials and Methods). Best-fitted parameters are $n = 2.1$, $K = 0.55$, and $r = 0.035$ with $R^2 = 1.0$. Thus, basal transcription occupies 3.4% of the maximal one.

source because to our knowledge all of the previous experiments estimated the effect of autorepression on total noise (15,16,21).

The strategy of noise decomposition developed in this study would, in principle, be applicable to other loop-containing biological networks such as those seen in metabolism and signal transduction irrespective of the signs of the loops. Model-based decomposition of noise for such a network would constitute a framework to understand noise-related properties of the network, and reveal parameter-independent aspects characteristic to the structure of the network. Subsequent experimental estimation of path and loop gains under physiological parameter sets will uncover parameter-dependent features for the effects of feedback loops. Understanding the structure- and parameter-dependent noise-related properties highlights the design principle that has guided the evolution of current loop-containing networks.

APPENDIX A: EFICIENCIES OF NOISE ATTENUATION BY AUTOREPRESSION

Here we prove theoretically that transcriptional autorepression attenuates fluctuations irrespective of its noise source except for a protein maturation reaction. Mathematically, this is equivalent to showing that all relevant loop gains are <1. We also prove that their efficiencies are ordered irrespective of parameter values.

First, we show that $\Xi_{\mathrm{mG}}>\Xi_{\mathrm{iG}}>1$ holds. From definition of loop gains, we have

$$\begin{aligned}\Xi_{\mathrm{mG}}-\Xi_{\mathrm{iG}} &= -H_{1,3}(1-T^{\mathrm{R}}_{1,2:3}-T^{\mathrm{R}}_{3,2:1})\\ &\quad -H_{1,2}(1-T^{\mathrm{R}}_{3,2:1}+T^{\mathrm{R}}_{1,2:3}C)+T^{\mathrm{R}}_{1,2:3}C+H_{1,3}R^{3}_{1,2},\end{aligned}$$

where we define $C=H_{1,3}R^{3}_{1,2}-H_{1,2}$. Since $H_{1,2}=(k_4/k_3)H_{1,3}$ holds in our model, we have $C=-H_{1,2}(k_1+k_3)/(k_1+k_3+k_4)>0$. Furthermore, we have $1-T^{\mathrm{R}}_{1,2:3}-T^{\mathrm{R}}_{3,2:1}>1-T_{1,3}-T_{3,1}=0$. Thus, $\Xi_{\mathrm{mG}}>\Xi_{\mathrm{iG}}$ holds. Since $\Xi_{\mathrm{iG}}>1$ is evident, $\Xi_{\mathrm{mG}}>\Xi_{\mathrm{iG}}>1$ is proved.

From definition of loop gains and the relation $H_{1,2}=(k_4/k_3)H_{1,3}$ we have

$$\frac{\Xi_{\mathrm{mG}}}{\Xi_{\mathrm{all}}}=\frac{\Xi_{\mathrm{all}}+H_{1,3}T^{\mathrm{R}}_{1,2:3}C}{\Xi_{\mathrm{all}}}.$$

As shown above, $C>0$ holds. Thus, $(\Xi_{\mathrm{mG}}/\Xi_{\mathrm{all}})<1$ is proved. Hence, $(\Xi_{\mathrm{iG}}/\Xi_{\mathrm{all}})<1$ and $(1/\Xi_{\mathrm{all}})<1$ also hold.

Finally, we show that $G^{\mathrm{up}}*P^{\mathrm{up}}<(1/\Xi_{\mathrm{all}})(1,1,1,1,1)*P^{\mathrm{up}}$ holds. If this inequality holds, it is natural to conclude that upstream noise is more efficiently attenuated by autorepression than mRNA noise. The inequality is equivalent to the following one:

$$\begin{aligned}&\left(1-\frac{1}{T_{1,4}R^{2}_{3,4}},1,1,1,1+\frac{k_4}{k_3}T_{3,1}R^{1,4}_{2,4}\right)\\ &\quad\cdot(T_{1,3}R^{2}_{3,4}R^{1,2}_{2,4},T_{1,3}R^{2}_{3,4}R^{1,2}_{2,4}R^{3,4}_{1,2},R^{2}_{3,1},R^{2}_{2,4},1)>0,\end{aligned}$$

where we define $R^{\mathrm{i,j}}_{\mathrm{k,l}}=(1/\tau_{\mathrm{i}}+1/\tau_{\mathrm{j}})/(1/\tau_{\mathrm{k}}+1/\tau_{\mathrm{l}})$.

The absolute value of the only negative term $-(T_{1,3}R^{1,2}_{2,4})/(T_{1,4})$ can be easily shown to be less than $(1,1+(k_4)/(k_3)T_{3,1}R^{1,4}_{2,4})*(R^{2}_{2,4},1)$. Thus, $G^{\mathrm{up}}\cdot P^{\mathrm{up}}<(1/\Xi_{\mathrm{all}})(1,1,1,1,1)\cdot P^{\mathrm{up}}$ is proved.

Hence, the above statements for efficiencies of noise attenuation as well as their ordering are proved.

APPENDIX B: SIMPLIFICATION OF THE FULL KINETIC MODEL

In our full kinetic model, the maturation of GFP protein was explicitly modeled. In most of theoretical analysis, however, the maturation is often abbreviated for simplicity by assuming that the maturation process is faster than other biochemical processes.

When the maturation is fast enough to be ignored, namely, $k_4\to\infty$, then the path and loop gains are simplified as

$$\begin{aligned}P^{\mathrm{up}} &= H^{2}_{1,4}(T^{\mathrm{R}}_{3,1:4}T_{1,3},0,T_{3,1}T_{1,4},0,0)\langle x_4\rangle^{-1},\\ P^{\mathrm{mRNA}} &= T_{3,1}\langle x_1\rangle^{-1},\\ P^{\mathrm{im}} &= \frac{1}{2}\langle x_3\rangle^{-1},\\ P^{\mathrm{matu}} &= 0,\\ P^{\mathrm{dec}} &= \frac{1}{2}\langle x_3\rangle^{-1}.\\ G^{\mathrm{up}} &= \frac{1}{\Xi_{\mathrm{all}}\Xi_{\mathrm{up}}}(1,1,1,1,1+H_{1,3}T_{3,4}T_{1,3}),\\ G^{\mathrm{mRNA}} &= \frac{1}{\Xi_{\mathrm{all}}},\\ G^{\mathrm{im}} &= \frac{\Xi_{\mathrm{iG}}}{\Xi_{\mathrm{all}}},\\ G^{\mathrm{matu}} &= 1,\\ G^{\mathrm{dec}} &= \frac{\Xi_{\mathrm{mG}}}{\Xi_{\mathrm{all}}},\end{aligned}$$

where Ξ_{all}, Ξ_{iG}, Ξ_{mG}, and Ξ_{up} are also simplified as follows:

$$\begin{aligned}\Xi_{\mathrm{all}} &= 1-H_{1,3},\\ \Xi_{\mathrm{iG}} &= \Xi_{\mathrm{mG}}=1-H_{1,3}T_{3,1},\\ \Xi_{\mathrm{up}} &= 1-H_{1,3}T_{3,4}T_{1,4}.\end{aligned}$$

By excluding zero elements from P^{up}, the above path and loop gains are further simplified as follows:

$$\begin{aligned}P^{\mathrm{up}} &= H^{2}_{1,4}(T^{\mathrm{R}}_{3,1:4}T_{1,3}+T_{3,1}T_{1,4})\langle x_4\rangle^{-1},\\ P^{\mathrm{mRNA}} &= T_{3,1}\langle x_1\rangle^{-1},\\ P^{\mathrm{down}} &= \langle x_3\rangle^{-1},\\ G^{\mathrm{up}} &= \frac{1}{\Xi_{\mathrm{all}}\Xi_{\mathrm{up}}},\\ G^{\mathrm{mRNA}} &= \frac{1}{\Xi_{\mathrm{all}}},\end{aligned}$$

$$G^{\mathrm{down}} = \frac{\Xi_{\mathrm{down}}}{\Xi_{\mathrm{all}}}.$$

By using these path and loop gains, CV^2_{mG} is represented as follows:

$$CV^2_{\mathrm{mG}} = \sum_{s\in\{\mathrm{up,mRNA,down}\}} G^s \cdot P^s.$$

The proof of the source-independent noise attenuation is much easier with this simplified model than the original full model because $G^{\mathrm{up}}<1$, $G^{\mathrm{mRNA}}<1$, and $G^{\mathrm{down}}<1$ evidently hold.

Not only the maturation process but also mRNA synthesis and degradation are sometimes abbreviated to obtain simple analytic results. If we furthermore assume that the decay rate of mRNA, k_1, is large, and one molecule of mRNA produces b molecules of proteins on average, we can have the following expression:

$$\begin{aligned}
P^{\mathrm{up}} &= H^2_{1,4}T_{3,4}\langle x_4\rangle^{-1},\\
P^{\mathrm{mRNA}} &= b\langle x_3\rangle^{-1},\\
P^{\mathrm{down}} &= \langle x_3\rangle^{-1},\\
G^{\mathrm{up}} &= \frac{1}{\Xi_{\mathrm{all}}\Xi_{\mathrm{up}}},\\
G^{\mathrm{mRNA}} &= \frac{1}{\Xi_{\mathrm{all}}},\\
G^{\mathrm{down}} &= \frac{1}{\Xi_{\mathrm{all}}},\\
\Xi_{\mathrm{all}} &= 1 - H_{1,3},\\
\Xi_{\mathrm{up}} &= 1 - H_{1,3}T_{3,4}.
\end{aligned}$$

Thus, we have

$$\begin{aligned}
CV^2_{\mathrm{mG}} &= \sum_{s\in\{\mathrm{up,mRNA,down}\}} G^s \cdot P^s\\
&= \frac{(1+b)}{\Xi_{\mathrm{all}}}\langle x_3\rangle^{-1} + \frac{H^2_{1,4}}{\Xi^2_{\mathrm{all}}}\frac{\Xi_{\mathrm{all}}T_{3,4}}{\Xi_{\mathrm{up}}}\langle x_4\rangle^{-1}.
\end{aligned}$$

If we define $H^{\mathrm{P}}_{21} = H_{1,4}$, $H^{\mathrm{P}}_{22} = \Xi_{\mathrm{all}}, H^{\mathrm{P}}_{11} = 1$, $\tau^{\mathrm{P}}_1 = \tau_4, \tau^{\mathrm{P}}_2 = \tau_3, \langle n^{\mathrm{P}}_1\rangle = \langle x_4\rangle, \langle n^{\mathrm{P}}_2\rangle = \langle x_3\rangle$, our reduced equation is equivalent to Eq. 1 in Paulsson (19):

$$\frac{\sigma^2_2}{\langle n^{\mathrm{P}}_2\rangle^2} \approx \frac{1+b}{\langle n^{\mathrm{P}}_2\rangle H^{\mathrm{P}}_{22}} + \frac{\sigma^2_1}{\langle n^{\mathrm{P}}_1\rangle^2}\frac{(H^{\mathrm{P}}_{21})^2}{(H^{\mathrm{P}}_{22})^2}\frac{H^{\mathrm{P}}_{22}/\tau^{\mathrm{P}}_2}{H^{\mathrm{P}}_{11}/\tau^{\mathrm{P}}_1 + H^{\mathrm{P}}_{22}/\tau^{\mathrm{P}}_2},$$

where the intrinsic-noise term is slightly changed to include the effect of the burst size, b. In addition, since $\Xi_{\mathrm{all}} = 1 - H_{1,3}$ is identical to $1+|T(0)|$ in Eq. 16 of Simpson et al. (20) and $1 - T(0)$ in Eq. 27 of Cox et al. (22), our full kinetic model can also consistently explain the result obtained by the frequency domain analysis.

APPENDIX C: EXPERIMENTAL ESTIMATION OF PATH AND LOOP GAINS

From the expression of path gains and loop gains (see Theory), we demonstrate several features of fluctuations that allow us to experimentally estimate some loop and path gains by using transcription and translation rates as control parameters.

First, both transcription and translation rates affect path gains only implicitly via the average copy number of mRNA transcripts and the mature protein molecules.

Second, path gains from upstream, mRNA, and downstream noise sources linearly depend on $\langle x_4\rangle^{-1}$, $\langle x_1\rangle^{-1}$, and $\langle x_3\rangle^{-1}$, respectively. Under no autorepression, $\langle x_1\rangle$ and $\langle x_3\rangle$ linearly depend on the transcription rate and only $\langle x_3\rangle$ linearly depends on the translation rate. Hence, when autorepression does not work, i), the path gain from the upstream noise source remains constant by altering transcription and/or translation rates, ii), the path gain from mRNA synthesis and decay remains constant by altering a translation rate while it changes by altering a transcription rate, and iii), the path gain from the downstream noise source changes by altering transcription or translation rates. By using these different dependencies of the path gains on transcription and translation rates (Table 3), we can experimentally estimate the relative contributions of the three noise sources to fluctuations of mature proteins under no autorepression.

Third, loop gains depend on copy numbers of system components or on transcription and translation rates only through the logarithmic gains $H_{1,2}$ and $H_{1,3}$. $H_{1,2}$ and $H_{1,3}$ depend on the copy number of upstream components, $\langle x_4\rangle$, and the total copy numbers of TetR:GFP proteins, $\langle x_2\rangle+\langle x_3\rangle$. In our experiments, $\langle x_4\rangle$ is assumed to be constant by any alteration of transcription or translation rates. Furthermore, the ratio of the copy number of immature proteins to that of mature proteins is also constant in our experiment because the ratio is determined only by the rate constant of maturation. Thus, all loop gains remain unchanged as long as $\langle x_3\rangle$ is kept constant.

Taken together, simultaneous alteration of transcription and translation rates under constant $\langle x_3\rangle$ affects only the path gain for mRNA noise, and keeps the other path gains (Table 3) as well as all loop gains unchanged. Thus, if fluctuations of the mature proteins are compared under the different sets of transcription and translation rates with the copy number of the mature proteins kept constant, the difference in the values of CV^2 originates purely from the change in the path gain for the mRNA noise. Since the value of each path gain for given $\langle x_3\rangle$ can be obtained from the experiments under no autorepression, the loop gain for mRNA noise can be estimated as described in the main text.

APPENDIX D: ESTIMATION OF THE EFFCT CAUSED BY THE DIFFERENCE IN THE GENE COPY NUMBER

In our experimental system, binding of repressor proteins to operators is competitive with loading of the RNA polymerase holoenzyme on the promoter. Modulation of transcription rates by altering the promoter sequence would therefore change the function that represents autorepression. As an alternative, we transferred the autorepression module from the *kup* locus near the replication origin to the *galK* locus near the replication terminus. Because the average copy number of the gene, D_0, is different between the two gene loci, the copy number of the free repressor molecules could be different despite the identical copy number of the total repressor molecules, especially when the total copy number is very low. Here, we estimate this effect under the set of parameters determined from the autorepression curve.

The steady-state average copy number of derepressed genes, D_{f}, satisfies the following relation,

$$-b_1 x^{\mathrm{n}} D_{\mathrm{f}} + b_{-1} D_{\mathrm{b}} = 0,$$

TABLE 3 Dependency of path gains on individual noise sources

Path gains under no autorepression	$1^{\mathrm{T}} * P^{\mathrm{up}}$	P^{mRNA}	$1^{\mathrm{T}} * P^{\mathrm{down}}$
Dependency on the copy number	$\langle x_4\rangle^{-1}$	$\langle x_1\rangle^{-1}$	$\langle x_3\rangle^{-1}$
Dependency on a transcription rate	No	Yes	Yes
Dependency on a translation rate	No	No	Yes

where D_b and x represent the steady-state average copy numbers of repressed genes and free repressors, respectively, b_1 and b_{-1} denote the association and dissociation rate constants, respectively, and n is the Hill coefficient. The transcription rate, f, then can be described as $f = k_r(D_f + r_0 D_0)$, where k_r is the rate of transcription from one unrepressed gene, and r_0 represents leaky initiation of transcription that occurs irrespective of the presence of the excess amount of repressor proteins. The copy number of the free repressors is represented as $x = x_0 - D_b$, where x_0 is the total copy number of the repressors. If the copy number of the repressors is sufficiently large, we can approximate x as $x \equiv x_0$. Our aim is to estimate the influence of this approximation on relative errors of f and its logarithmic gain. Let D_f^{app} be the steady-state average copy number of derepressed genes under the approximation. We also define $P_f^{app} = D_f^{app}/D_0$, $P_f = D_f^{app}/D_0$, $B = b_{-1}/b_1/D_0$, and $y = x_0/D_0$. With these values, f and f^{app} are described as $f = k_r D_0(P_f + r_0)$ and $f^{app} = k_r D_0(P_f^{app} + r_0)$. We have a simple explicit solution for P_f^{app} as $P_f^{app}(y) = B^n/B^n + y^n$ whereas the analytical solution of P_f becomes complicated even for n=2. We introduce ε defined as $\varepsilon = B/Y$. We take $\varepsilon \in \{10^{-1}, 10^{1}\}$ as an appropriate range of ε because P_f^{app} and its logarithmic gain change most drastically when ε is close to 1, and autorepression in our experimental system is neither too loose nor too tight. For $y>1$ and $\varepsilon \in \{10^{-1}, 10^{1}\}$, we numerically calculated the relative approximation errors of the transcription rate $|f^{app} - f|/f^{app}$ and the logarithmic gain, $|df^{app}/dy/f^{app} - df/dy/f|/(df^{app}/dy/f^{app})$ by using experimentally determined parameters (Fig. 4 *C*). To conduct the calculation, we used $r_0 = 0.035$, which was estimated from our experiment. It should be noted that the errors of the transcription rate and its logarithmic gain is independent of k_r.

The average copy number of fluorescent repressors in the HOE233 strain under autorepression was estimated as 68 if we assume that the downstream fluctuations obeys a Poisson distribution as in our model. We can estimate the copy number of non-fluorescent repressor from the reported maturation rate of EGFP ($t_{1/2}$ = 65 min) (32) and the rate of cell division in our experiment ($t_{1/2}$ = 40 min). Since cellular fluorescence was observed to increase by about 10% during on ice incubation before microscopic measurement, we compensated the estimation by this factor and obtained 162 as the total copy number of repressors. Since the copy number of the gene in individual *E. coli* cells ranges from 1 to 8 depending on the gene locus and growth condition, the y value is estimated as higher than 20. Fig. 4 shows that the relative errors of the transcription rate and the logarithmic gain are at most no more than 6% and 14%, and would be lower than these values for most of the cells. Thus, the approximation is valid in our experiment.

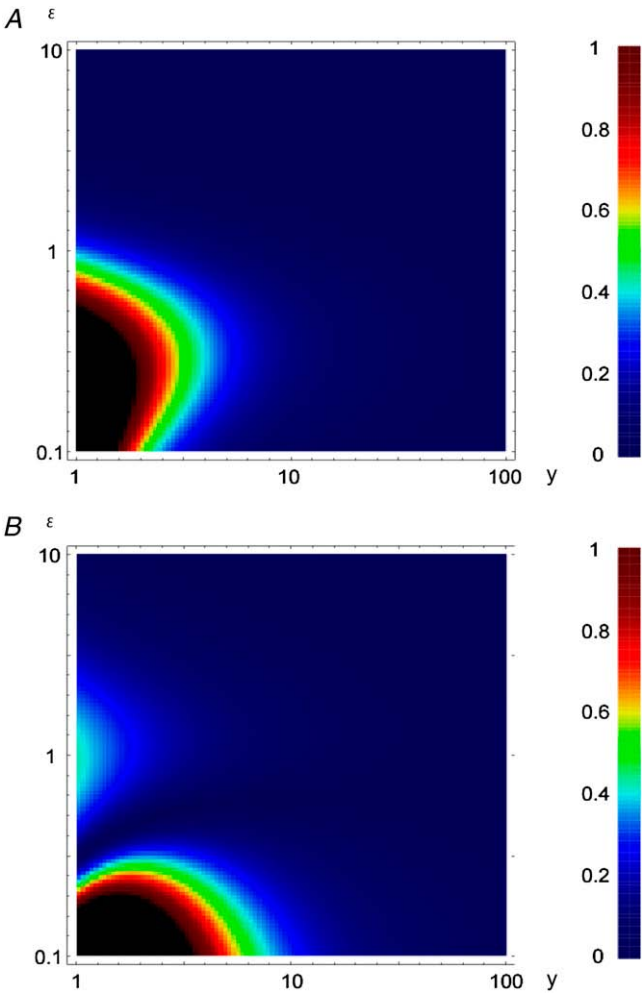

FIGURE 4 (*A*) Relative errors of the transcription rate. (*B*) Relative errors of the logarithmic gain.

SUPPLEMENTARY MATERIAL

To view all of the supplemental files associated with this article, visit www.biophysj.org.

We thank Attila Becskei and Hermann Bujard for generously providing plasmids, and Hideo Iwasaki for helpful discussion.

REFERENCES

1. Houchmandzadeh, B., E. Wieschaus, and S. Leibler. 2002. Establishment of developmental precision and proportions in the early Drosophila embryo. *Nature*. 415:798–802.
2. Ozbudak, E. M., M. Thattai, I. Kurtser, A. D. Grossman, and A. van Oudenaarden. 2002. Regulation of noise in the expression of a single gene. *Nat. Genet*. 31:69–73.
3. Elowitz, M. B., A. J. Levine, E. D. Siggia, and P. S. Swain. 2002. Stochastic gene expression in a single cell. *Science*. 297:1183–1186.
4. Blake, W. J., M. Kærn, C. R. Cantor, and J. J. Collins. 2003. Noise in eukaryotic gene expression. *Nature*. 422:633–637.
5. Raser, J. M., and E. K. O'Shea. 2004. Control of stochasticity in eukaryotic gene expression. *Science*. 304:1811–1814.
6. Becskei, A., B. B. Kaufmann, and A. van Oudenaarden. 2005. Contributions of low molecule number and chromosomal positioning to stochastic gene expression. *Nat. Genet*. 31:69–73.
7. Rosenfeld, N., J. W. Young, U. Alon, P. S. Swain, and M. B. Elowitz. 2005. Gene regulation at the single-cell level. *Science*. 307:1962–1965.
8. Kaern, M., T. C. Elston, W. J. Blake, and J. J. Collins. 2005. Stochasticity in gene expression: from theories to phenotypes. *Nat. Rev. Genet*. 6:451–464.
9. Rao, C. V., D. M. Wolf, and A. P. Arkin. 2002. Control, exploitation and tolerance of intracellular noise. *Nature*. 420:231–237.
10. Raser, J. M., and E. K. O'Shea. 2005. Noise in gene expression: origins, consequences, and control. *Science*. 309:2010–2013.
11. Pedraza, J. M., and A. van Oudenaarden. 2005. Noise propagation in gene networks. *Science*. 307:1965–1969.
12. Thattai, M., and A. van Oudenaarden. 2001. Intrinsic noise in gene regulatory networks. *Proc. Natl. Acad. Sci. USA*. 98:8614–8619.
13. Swain, P. S., M. B. Elowitz, and E. D. Siggia. 2002. Intrinsic and extrinsic contributions to stochasticity in gene expression. *Proc. Natl. Acad. Sci. USA*. 99:12795–12800.
14. Thieffry, D., A. M. Huerta, E. Pérez-Rueda, and J. Collado-Vides. 1998. From specific gene regulation to genomic networks: a global analysis of transcriptional regulation in *Escherichia coli*. *Bioessays*. 20: 433–440.

15. Becskei, A., and L. Serreno. 2000. Engineering stability in gene networks by autoregulation. *Nature*. 405:590–593.

16. Dublanche, Y., K. Michalodimitrakis, N. Kümmerer, M. Foglierini, and L. Serrano. 2006. Noise in transcription negative feedback loops: simulation and experimental analysis. *Mol. Syst. Biol.* 2:41.

17. Tomioka, R., H. Kimura, T. J. Kobayashi, and K. Aihara. 2004. Multivariate analysis of noise in genetic regulatory networks. *J. Theor. Biol.* 229:501–521.

18. Morishita, Y., T. J. Kobayashi, and K. Aihara. 2005. Evaluation of the performance of mechanisms for noise attenuation in a single-gene expression. *J. Theor. Biol.* 235:241–264.

19. Paulsson, J. 2004. Summing up the noise in gene networks. *Nature*. 427:415–418.

20. Simpson, M. L., C. D. Cox, and G. S. Sayler. 2003. Frequency domain analysis of noise in autoregulated gene circuits. *Proc. Natl. Acad. Sci. USA*. 100:4551–4556.

21. Austin, D. W., M. S. Allen, J. M. McCollum, R. D. Dar, J. R. Wilgus, G. S. Sayler, N. F. Samatova, C. D. Cox, and M. L. Simpson. 2006. Gene network shaping of inherent noise spectra. *Nature*. 439:608–611.

22. Cox, C. D., J. M. McCollum, D. W. Austin, M. S. Allen, R. D. Dar, and M. L. Simpson. 2006. Frequency domain analysis of noise in simple gene circuits. *Chaos*. 16:026102.

23. Baumeister, R., V. Helbl, and W. Hillen. 1992. Contacts between Tet repressor and Tet operator revealed by new recognition specificities of single amino acid replacement mutants. *J. Mol. Biol.* 226:1257–1270.

24. Lutz, R., and H. Bujard. 1997. Independent and tight regulation of transcriptional units in *Escherichia coli* via the LacR/O, the TetR/O and AraC/I_1-I_2 regulatory elements. *Nucleic Acids Res.* 25:1203–1210.

25. McCarthy, J. E., W. Sebald, G. Gross, and R. Lammers. 1986. Enhancement of translational efficiency by the *Escherichia coli atpE* translational initiation region: its fusion with two human genes. *Gene*. 41:201–206.

26. Olins, P. O., and S. H. Rangwala. 1989. A novel sequence element derived from bacteriophage T7 mRNA acts as an enhancer of translation of the *lacZ* gene in *Escherichia coli*. *J. Biol. Chem.* 264:16973–16976.

27. Gardner, T. S., C. R. Cantor, and J. J. Collins. 2000. Construction of a genetic toggle switch in *Escherichia coli*. *Nature*. 403:339–342.

28. Datsenko, K. A., and B. L. Wanner. 2000. One-step inactivation of chromosomal genes in *Escherichia coli* K-12 using PCR products. *Proc. Natl. Acad. Sci. USA*. 97:6640–6645.

29. van Kampen, N. G. 1997. Stochastic Processes in Physics and Chemistry. Elsevier Science, North-Holland, Amsterdam.

30. Elf, J., and M. Ehrenberg. 2003. Fast evaluation of fluctuations in biochemical networks with the linear noise approximation. *Genome Res.* 13:2475–2484.

31. Reid, B. G., and G. C. Flynn. 1997. Chromophore formation in green fluorescent protein. *Biochemistry*. 36:6786–6791.

32. Evdokimov, A. G., M. E. Pokross, N. S. Egorov, A. G. Zaraisky, I. V. Yampolsky, E. M. Merzlyak, A. N. Shkoporov, I. Sander, K. A. Lukyanov, and D. M. Chudakov. 2006. Structural basis for the fast maturation of *Arthropoda* green fluorescent protein. *EMBO Rep.* 7: 1006–1012.

33. Shibata, T., and K. Fujimoto. 2005. Noisy signal amplification in ultrasensitive signal transduction. *Proc. Natl. Acad. Sci. USA*. 102: 331–336.